Economic Geology
Vol. 93, 1998, pp. 201–215

Deposition of Gold in Carlin-Type Deposits: The Role of Sulfidation and Decarbonation at Twin Creeks, Nevada

DAVID P. STENGER,* STEPHEN E. KESLER,†

Department of Geological Sciences, University of Michigan, Ann Arbor, Michigan 48109

DEAN R. PELTONEN,** AND CHARLES J. TAPPER***

Santa Fe Pacific Gold Corporation, Twin Creeks Mine, P.O. Box 69, Golconda, Nevada 89414

Abstract

We report here an investigation of the distribution of Au, As, Sb, Hg, carbonates, K-Al silicates, and pyrite in the Twin Creeks Carlin-type gold deposit. The main objective of the study was to determine the nature and degree of correlation among these variables and use them to identify the process(es) that deposited gold. The study focused on deposit-scale variations in these parameters and was based, in part, on data from two large geochemical databases that were prepared by mine staff.

Country rocks at Twin Creeks include Ordovician-age interlayered calcareous shales and mafic igneous rocks, the overlying Leviathan allochthon, and the Pennsylvanian-Permian Etchart Formation that was deposited unconformably over these rocks. Most gold values are found in calcareous shales in the Ordovician sequence and in limestones in the Etchart Formation, although *not* all layers contain the same amount of gold. Strongest gold mineralization is not adjacent to faults but its general form and distribution suggest that gold-bearing solutions gained access to favorable layers along the faults. In the Ordovician sequence, gold values are highest in shales that have undergone maximum dissolution of carbonate minerals. Petrographic study shows that some gold is associated with adularia, but deposit-scale comparisons do not show a consistent relation between K/Al ratios and gold values. The distribution of antimony is similar to that of gold, whereas mercury is more concentrated than gold, and arsenic is more widely dispersed than gold.

The relation between gold, iron, and sulfide sulfur values shows that mineralization is concentrated in rocks that have gained sulfur, *but not iron*, to form gold-bearing arsenian pyrite. Thus, these rocks have undergone sulfidation rather than pyritization. The iron that underwent sulfidation came largely from preore, diagenetic(?) ferroan dolomite and was released into solution by decarbonation, a common form of alteration associated with Carlin-type deposits. The results of this study suggest that wall-rock iron content and decarbonation processes which liberate this iron are the most important factors controlling formation of Carlin-type gold deposits. New deposits should be sought where stratigraphic units containing abundant ferroan dolomite are cut by favorable structures.

Introduction

DESPITE advances in our understanding of the geology and mineralogy of Carlin-type deposits and the chemistry of their ore fluids (Radtke et al., 1980; Rye, 1985; Bakken et al., 1989; Hofstra et al., 1991; Kuehn and Rose, 1992, 1995; Arehart et al., 1993; Cline et al., 1997), we lack information on the process that causes gold to deposit. One of the main factors limiting progress toward this goal is the lack of quantitative information on the relation between gold values and other elemental and mineralogic features at the scale of an entire deposit. In this study, we have combined geologic and petrographic observations with information from two large geochemical databases to investigate these relations at the Twin Creeks Carlin-type deposit near Winnemucca, Nevada (Fig. 1).

Twin Creeks is a combination of two formerly separate gold mines, Chimney Creek and Rabbit Creek, and was the third largest operating gold mine in the United States at the time of this study, with annual production of about 450,000 oz. Proven and probable reserves on December 31, 1996, included 150 million tons averaging 0.073 oz/t (Newmont Mining Company Twin Creeks mine field trip guide, October, 1997). Chimney Creek is comprised of the Vista and Discovery pits (Fig. 1), which are north of the much larger Rabbit Creek pit, which is called the "Megapit." Some aspects of mineralization and alteration at Chimney Creek and the Megapit have been described previously by Bloomstein et al. (1990), Osterberg (1990), Groff (1996), and Groff et al. (1997) and are discussed below.

Geology of the Twin Creeks Mine

The Twin Creeks mine is located on the eastern flank of the Osgood Mountains just west of the Pinson, Preble, and Getchell gold deposits, although it is hosted, in part, by different rocks. The base of the exposed section at Twin Creeks consists of Ordovician-age interlayered sedimentary and igneous rocks and an overthrust wedge known as the "Leviathan allochthon." These are overlain unconformably by the Pennsylvanian-Permian Etchart formation, which is covered, in turn, by the Golconda allochthon. The entire section is covered by alluvium that thickens toward the south.

Stratigraphy of the mine area

Ordovician-age rocks in the Twin Creeks mine consist of dolomitic to calcareous, black shale and siltstone with inter-

† Corresponding author: email, skesler@umich.edu
* Present address: Golden Star Resources, 1700 Lincoln Street, Suite 1950, Denver, Colorado 80203
** Present address: Newmont Exploration Ltd., P.O. Box 669, Carlin, Nevada 89822
*** Present address: Barrick Gold Exploration, Inc., 293 Spruce Road, Elko, Nevada 89803

0361-0128/98/1966/201-15$6.00

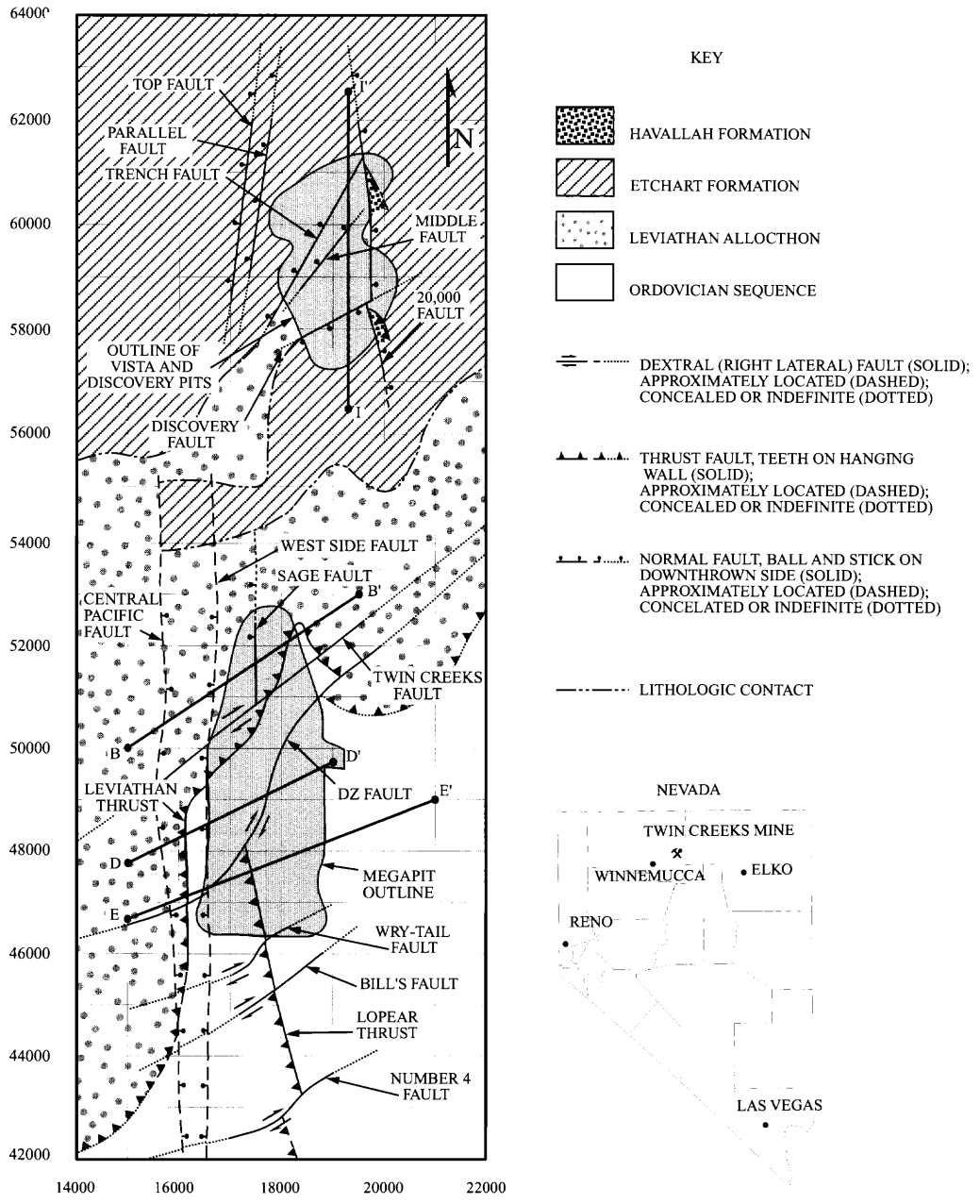

FIG. 1. Geologic and structural map of the Rabbit Creek mine area based on mapping by Santa Fe personnel showing location of the Chimney Creek (Vista and Discovery pits) and Twin Creeks (Megapit) mining areas (shaded), along with locations of cross sections that are shown in later figures. Inset shows location of mine in Nevada. Distances on mine coordinates are in feet. Additional cross sections, not shown here, are available in Stenger (1996).

layered basaltic and possibly ultramafic tuffs, sills, and flows. These rocks were originally correlated with the Ordovician Comus Formation that is exposed in the Osgood Mountains (Bloomstein et al., 1990), although structural relations observed in recent deep drilling at Twin Creeks suggest that they correlate with the Early Ordovician Valmy Formation. Bloomstein et al. (1990) divided this Ordovician sequence into upper and lower members, which are separated by a distinctive igneous layer known as the main sill. The upper member contains up to 70 percent basalt flows and sills, whereas the lower member contains less than 30 percent and is dominated by black shale that was deposited in an anoxic, deep-water environment. The presence of basalt flows and volcaniclastic rocks in this sequence indicates a nearby volcanic center, possibly a seamount (Bloomstein et al., 1990). The Ordovician sequence is overthrust at a low angle by rocks of possible Devonian age in the Leviathan allochthon. The lower part of the Leviathan sequence consists largely of tuffaceous sediments with thin layers of shale and chert; the upper part contains basalt with abundant pillow structures indicating submarine emplacement.

Unconformably overlying the Leviathan allochthon, and clearly in depositional contact, is the Pennsylvanian-Permian Etchart formation. The Etchart formation here probably in-

cludes the Middle Pennsylvanian Highway and Late Pennsylvanian-Early Permian Antler Peak formations, which are part of the marine overlap assemblage that was deposited in central Nevada during and after the Antler orogeny (Hotz and Willden, 1964; Stewart, 1980; Osterberg, 1990). The Etchart formation is about 600 m thick at Twin Creeks and has been divided into upper, middle, and lower members. The upper member consists of calcareous siltstone that grades locally into fine-grained sandstone. The middle member consists of silty to sandy limestones with minor chert-pebble conglomerate and micritic and fossiliferous limestone. It includes an extensive paleokarst system with caverns up to 3 m high that are filled by blocks of Middle Etchart Limestone in a matrix of fine-grained, calcareous sandstone and siltstone. The lower member includes calcareous and noncalcareous sandstones, as well as chert-pebble conglomerates.

Structure of the mine area

Megapit area: In the Megapit area, the Ordovician sequence has been deformed into a northwest-trending fold system known as the "Conelea anticline," with a known strike length of about 4.8 km. This fold system formed prior to gold mineralization and in the pit area is cut by the right-lateral TC and DZ faults that trend northeast-southwest, dip steeply to the northwest, and divide the mine into north, central, and south fault blocks (Fig. 1). In the north fault block, the upper limb of the Conelea anticline and the Leviathan allochthon are dropped into a graben formed by the north-striking West Side and Central Pacific faults (Fig. 2A). In this same area, the north-south Sage fault cuts mineralization, parts of the upper fold limb, and the Leviathan allochthon with less than 15 m of normal displacement. Along the DZ fault, the Cone-

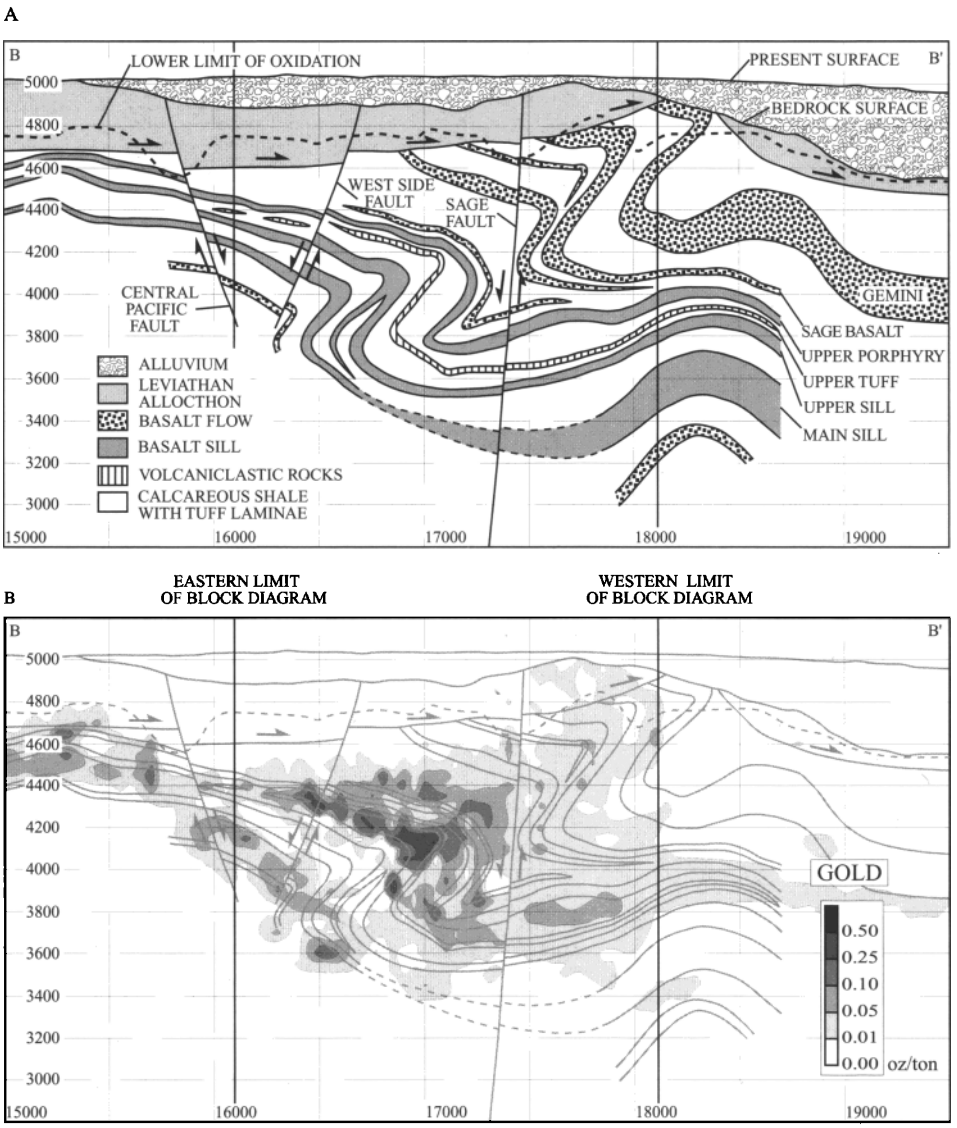

FIG. 2. Geologic cross section B-B' through the Megapit area, looking north, showing location of major structures and stratigraphic units (A) and distribution of gold grades (B). Note lack of mineralization in sediments between the main and upper sills. Distances on mine coordinates and elevations are in feet.

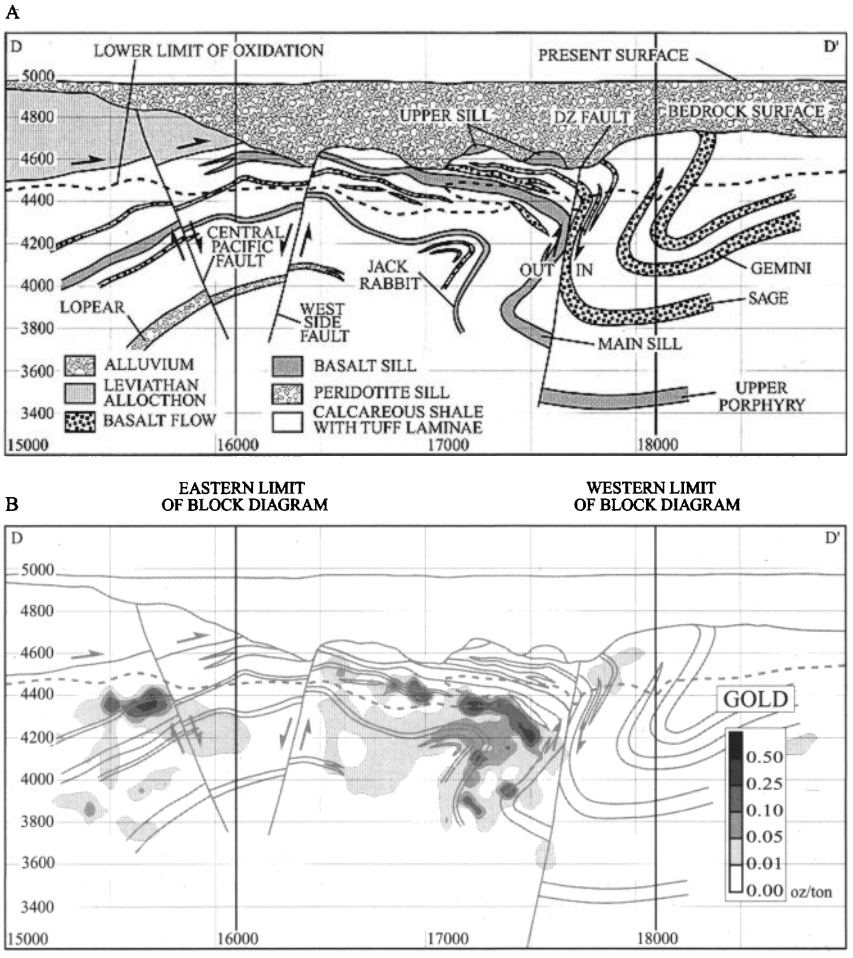

FIG. 3. Geologic cross section D-D′ through the Megapit area, looking north, showing location of major structures and stratigraphic units (A) and distribution of gold grades (B). Note lack of mineralization in sediments between the main and upper sills. Distances on mine coordinates and elevations are in feet.

lea anticline has been offset by right-lateral movement that moved the middle and lower limbs of the fold in the southern fault block against the middle and upper limbs of the fold in the central fault block (Fig. 3A). Figures 3A and 4A also show that alluvium thickens toward the southern end of the Megapit. As a result, most of the Leviathan allochthon has been eroded from the central fault block east of the West Side fault. In the southern part of the central fault block, the upper part of the fold has also been extensively eroded, and in the south fault block, only the lower part of the fold system remains.

The Lopear thrust fault intersects the fold system along the axial plane of the western fold (Fig. 4A). Dislocation along the Lopear thrust increases to the south with scissorslike movement along the fault. The point at which the direction of apparent motion changes from reverse to thrust lies just to the south of section E-E′ (Fig. 4) and motion about this pivot caused the apparent reverse movement that is visible along the Lopear thrust in Figure 4A. The steeply dipping DZ fault in the western part of the section exhibits right-lateral movement that truncates marker units in the western fold limb. Although deep erosion in the southern part of the Megapit has removed most of the Leviathan overthrust sequence, the DZ fault also cuts the remains of this unit. Figure 4A shows how the DZ fault, the Lopear thrust, and the Leviathan allochthon have been dropped into the shallow graben formed by the West Side and Central Pacific faults.

All major structures in the Megapit area are associated with or are younger than the Devonian-Mississippian Antler orogeny. The oldest structures in the Megapit area are the Conelea fold system that deforms the Ordovician sequence and the Lopear thrust, both of which probably formed during the Antler orogeny. The Leviathan allochthon truncates upper parts of the fold system in Figure 2A, indicating that the allochthon postdates the folding. The major right-lateral faults in the Megapit also formed after folding of the Ordovician sequence. The unconformable contact of the Etchart formation on the Leviathan allochthon indicates that the thrust was emplaced prior to Pennsylvanian time. The West Side and Central Pacific faults can only be constrained to an age later than the Antler orogeny. These two faults displace parts of the upper fold limb, the Leviathan allochthon, and the Lopear thrust in the graben that they bound on the west side of the Megapit. Parts of the TC fault, the DZ fault, and other right-lateral faults are also faulted down into this graben. Although the West Side and Central Pacific faults could

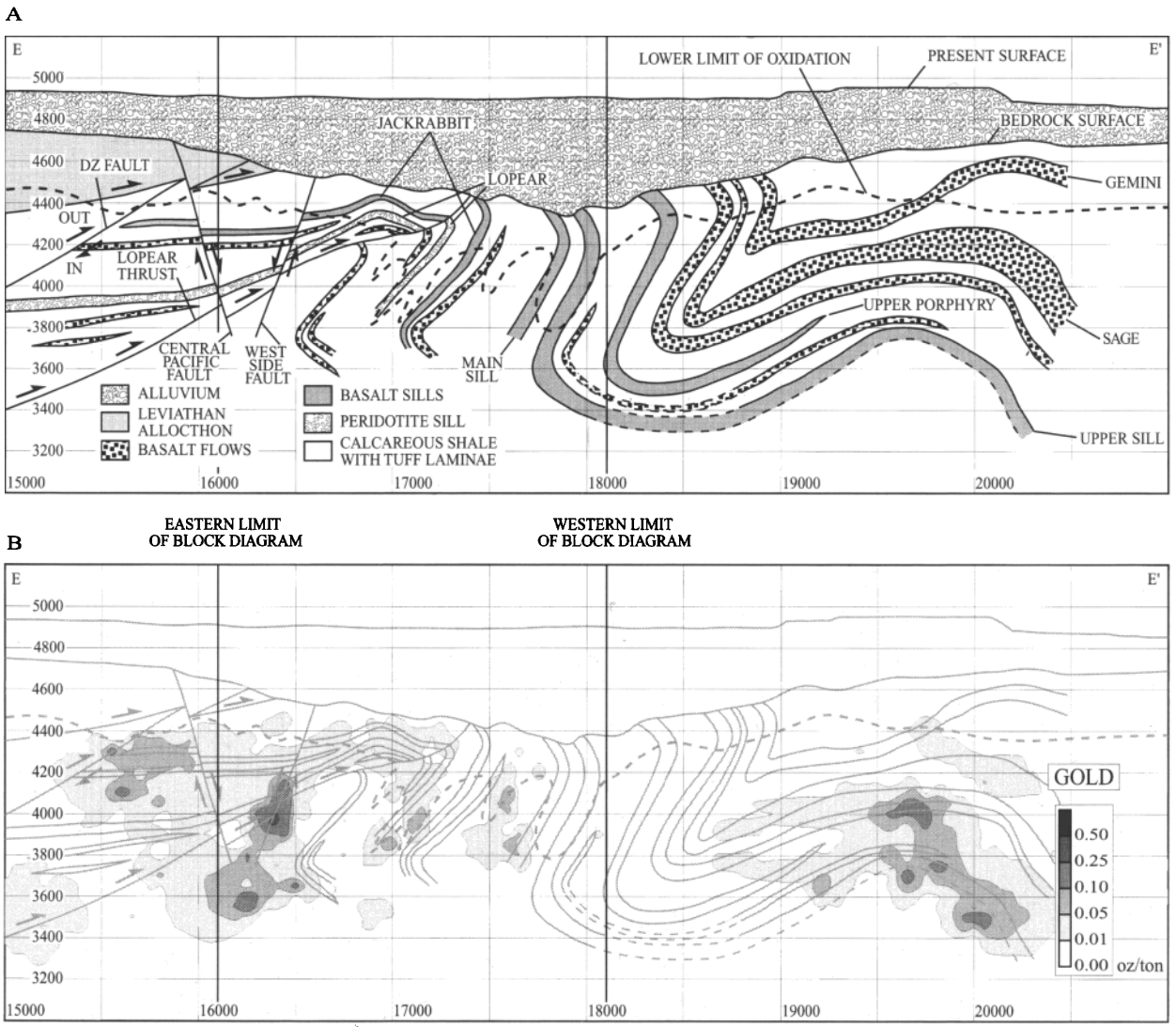

FIG. 4. Geologic cross section E-E′ through the Megapit area, looking north, showing location of major structures and stratigraphic units (A) and distribution of gold grades (B). Note that gold in the western part of the section is found largely above the upper sill. In the eastern part of the section, high gold grades are related to intersections of major faults; lower grade but more widespread mineralization occurs in sediments above the Lopear thrust. Distances on mine coordinates and elevations are in feet.

have formed after displacement of the fold by right-lateral motion, they could also reflect later reactivation and normal faulting along north-trending faults.

Chimney Creek area: In the Chimney Creek area, the Etchart formation and Leviathan allochthon dip gently to the north and are cut by the northeast-trending Discovery, Middle, and Trench faults, and the north-south-trending 20,000 fault, all of which display normal movement but no right-lateral movement (Fig. 5A). The southeast-dipping Discovery fault drops the lower Etchart formation downward by at least 130 m relative to the fault block to the north where the Leviathan allochthon is exposed. To the north, the northwest-dipping middle fault displaces the Etchart formation with an undefined amount of normal movement. In the northernmost part of Figure 5A, the Trench fault dips to the northwest and has dropped the Etchart formation by at least 75 m. East of the cross section shown in Figure 5A, the Etchart formation drops as much as 245 m on the west side of the 20,000 fault. Erosional remnants of the Golconda thrust represented by allochthonous Havallah Formation rocks are present along the east side of the 20,000 fault in this area (Fig.I 1) and are widespread north of the mine area.

Northeast-trending normal faults that cut the Chimney Creek area displace dikes and sills thought to be Cretaceous in age in the Etchart formation and could have formed during the Mesozoic Sevier orogeny (Osterberg, 1990). The Discovery fault cuts the 20,000 fault, which displaces the Havallah Formation that was emplaced during the Permian Sonoma orogeny, indicating that the Discovery and 20,000 faults are post-Permian in age. Few indications of the Sevier orogeny are observed at Twin Creeks and it is likely that this event reactivated older northeast-trending faults in underlying early Paleozoic rocks.

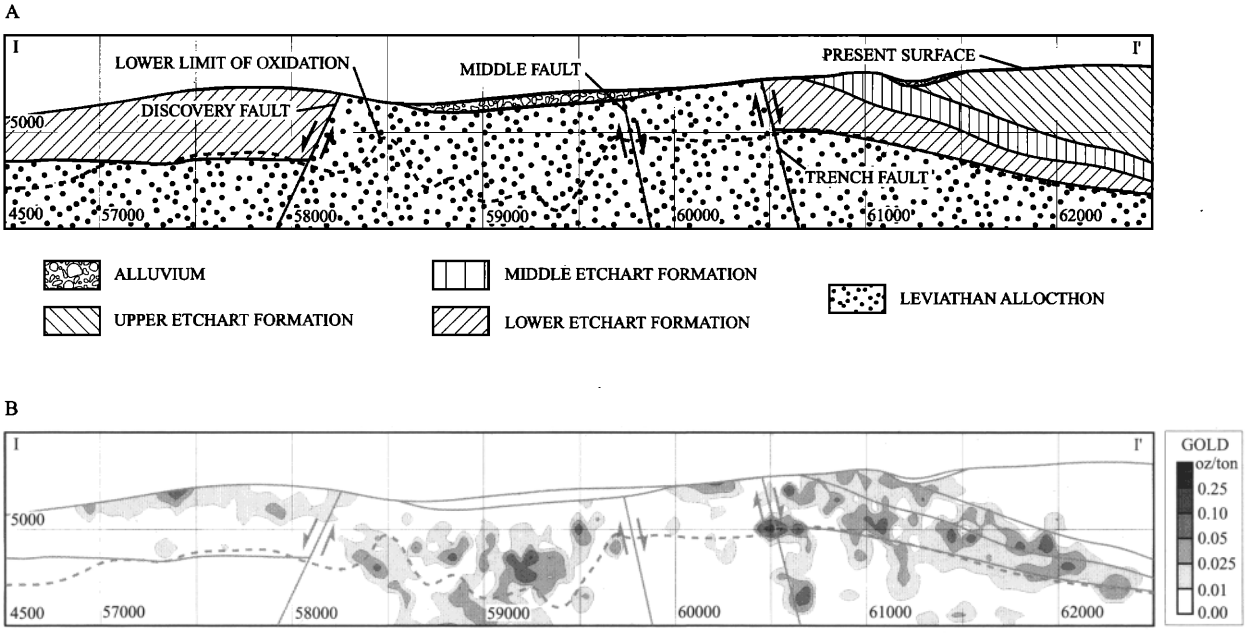

FIG. 5. Geologic cross section I-I' through the Chimney Creek area, looking east, showing location of major structures and stratigraphic units (A) and distribution of gold grades (B). In the northern part of the section, mineralization is largely restricted to the middle and lower Etchart formation. Similar patterns of mineralization were probably also present in the southern part of the section before the Middle Etchart was removed by erosion. Distances on mine coordinates and elevations are in feet.

Mineralization and alteration

Mineralization in the Chimney Creek area and parts of the southern Megapit consists largely of oxide ore. Abundant sulfide facies mineralization is exposed in the Megapit area north of the DZ fault and at depth to the south and can be divided into two general types (Simon et al., 1997; Hall et al., 1997). North of the TC fault, it consists largely of arsenian pyrite, whereas to the south, mineralization is richer in arsenic and contains arsenian pyrite along with locally abundant orpiment, realgar, and stibnite. Several different stages of mineralization have been recognized in both areas and they appear to be correlative. North of the TC fault, the first stage of mineralization contains base metals, arsenopyrite, and iron sulfides with quartz. A second stage consists of arsenian pyrite with high gold contents that is accompanied by K silicate minerals, including adularia to the north and illite to the south near the TC fault. Adularia from this stage of mineralization yields $^{40}Ar/^{39}Ar$ ages of 41.5 to 42.2 Ma and illite from the same stage of mineralization yields $^{40}Ar/^{39}Ar$ ages of 42.7 to 49.8 Ma (Groff et al., 1997; Hall et al., 1997). This was followed by introduction of quartz, stibnite, and minor visible gold, then two stages of arsenian pyrite separated by brecciation, and a final stage of minor realgar, orpiment, and stibnite. South of the DZ fault, the first stage of mineralization consisted of gold-bearing arsenian pyrite and abundant orpiment, which is thought to correlate with the second stage of arsenian pyrite north of the DZ fault. This was followed by more arsenian pyrite and a final stage of mineralization including orpiment, realgar, stibnite, and quartz. In general, orpiment, realgar, and stibnite are found at shallower levels of the deposit than arsenian pyrite, and the first stage of arsenian pyrite is found at deepest levels.

Pyrite textures at Twin Creeks range from euhedral and framboidal arsenic-free pyrite that formed during preore (diagenetic?) processes to small grains, aggregates, and overgrowths of arsenian pyrite that formed during mineralization (Simon et al., 1997). Ion microprobe analyses show that fine-grained arsenian pyrite is richest in gold, with contents of more than 1,400 ppm Au, and that gold contents of orpiment, stibnite, and realgar are insignificant. These mineralogical relations, along with information on XANES (X-ray adsorption near-edge spectroscopy) measurements that determine the oxidation state of gold in arsenian pyrite, are discussed in more detail by Simon et al. (1998a,b).

Distribution of Gold and Related Elements at Twin Creeks

Data from two large geochemical databases at Twin Creeks were used to delineate deposit-scale distributions of gold and other elements and determine their relation to important mineralogical and geologic features. The largest of these databases is comprised of 20-ft-bench composites from 5-ft assay intervals for hundreds of drill holes in the Megapit and Chimney Creek areas. Each composite contains data for Au, As, Sb, Hg, Fe, S (total and reduced), and C (total and carbonate), as well as information on lithology, degree of weathering, and location. The second database includes major element analyses of several hundred hand samples from drill core, with data for SiO_2, Al_2O_3, FeO, MgO, CaO, Na_2O, K_2O, P_2O_5, and TiO_2. Both of these databases are the property of the Santa Fe Pacific Gold Corporation (now Newmont Exploration Ltd.) and are not available for publication; all data in them were obtained by accepted analytical methods and they represent a "gold mine" of geochemical data for

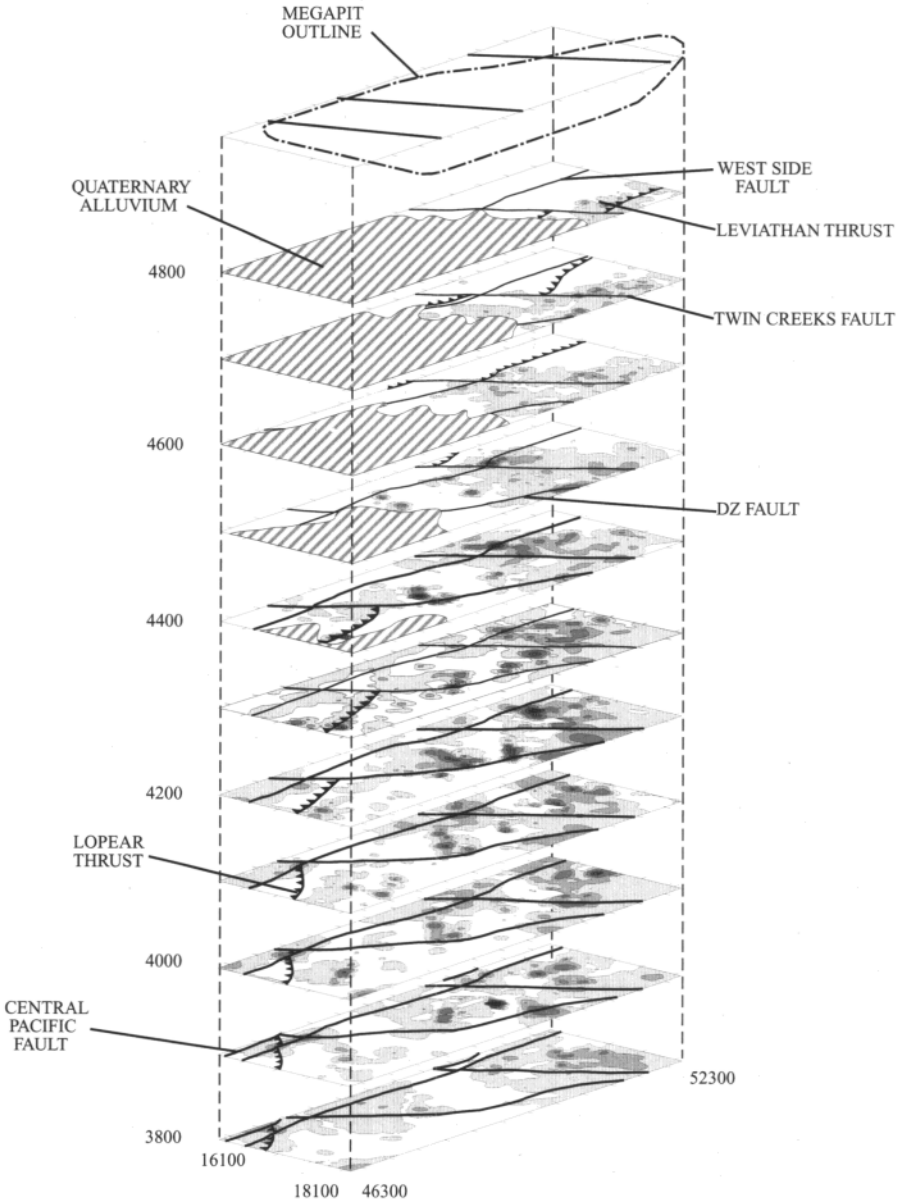

FIG. 6. lock diagram of the Megapit area showing the distribution of gold grades on 100-ft benches in relation to major faults. Top layer shows the outline of the Megapit and where the cross sections in Figures 2 to 4 intersect the limits of the block diagram. Note that most gold was deposited away from major faults, although local high-grade zones are close to faults. Distances on mine coordinates and elevations are in feet.

research. At the time of this study, software was not available to manipulate these databases to answer research-oriented questions, requiring us to develop computer procedures for projecting data onto cross section and plan views, and to portray the results in contour plots (Stenger, 1996). The distribution of drill holes and samples used to generate illustrations shown here can also be found in Stenger (1996).

Distribution of gold

The relation between gold values and structural and stratigraphic features at Twin Creeks is shown in cross sections (Figs. 2–5) and a multilayer block diagram for the Megapit area (Fig. 6). The overall impression gained from these plots is that major structural features provided important pathways for mineralizing solutions but that large amounts of gold were deposited away from the structures in favorable stratigraphic intervals.

For the Megapit, Figure 2B shows that gold in the folded Ordovician sequence is concentrated in sediments above the upper sill and below the main sill, but is lacking between them. Figure 3B shows a similar relationship; gold is concentrated below the main sill, but sediments between the upper and main sills are largely unmineralized. In addition, Figure 3B shows that high-grade mineralization is related locally to the Central Pacific fault. Ore-bearing and barren stratigraphic horizons in these two sections have undergone the same amount of folding, suggesting that fracturing and related permeability enhancement were not the only factors controlling the distribution of gold. In the southern part of the Megapit area, mineralization

is located in a broad anticlinal fold in sediments above the upper sill in the east and also in sediments below the main sill and above the Lopear thrust farther to the west (Fig. 4B). Figure 4B also shows that gold is related to intersections of the Lopear thrust and DZ fault with the West Side and Central Pacific faults, suggesting that increased permeability associated with faulting was a significant ore control here.

In the Chimney Creek area, the lower Etchart formation is the main gold host south of the Discovery fault, whereas mineralization is hosted by rocks of the Leviathan allochthon between the Discovery and Trench faults (Fig. 5). Gold in Etchart formation sediments forms lenticular pods that trend roughly parallel to the regional dip of the Etchart, and probably reflect stratigraphic control of mineralization (which we cannot investigate adequately because of the oxidized nature of the ore). These relations suggest that gold-bearing fluids migrated up the Trench and Discovery faults into permeable paleokarst zones in the middle Etchart formation and then down into the limey sandstone units of the lower Etchart formation. The middle Etchart formation has been eroded in the southern part of Chimney Creek (Fig. 5B), probably along with significant mineralization in these rocks. Gold in the Leviathan allochthon between the Discovery and Trench faults is largely unrelated to major structures, suggesting that

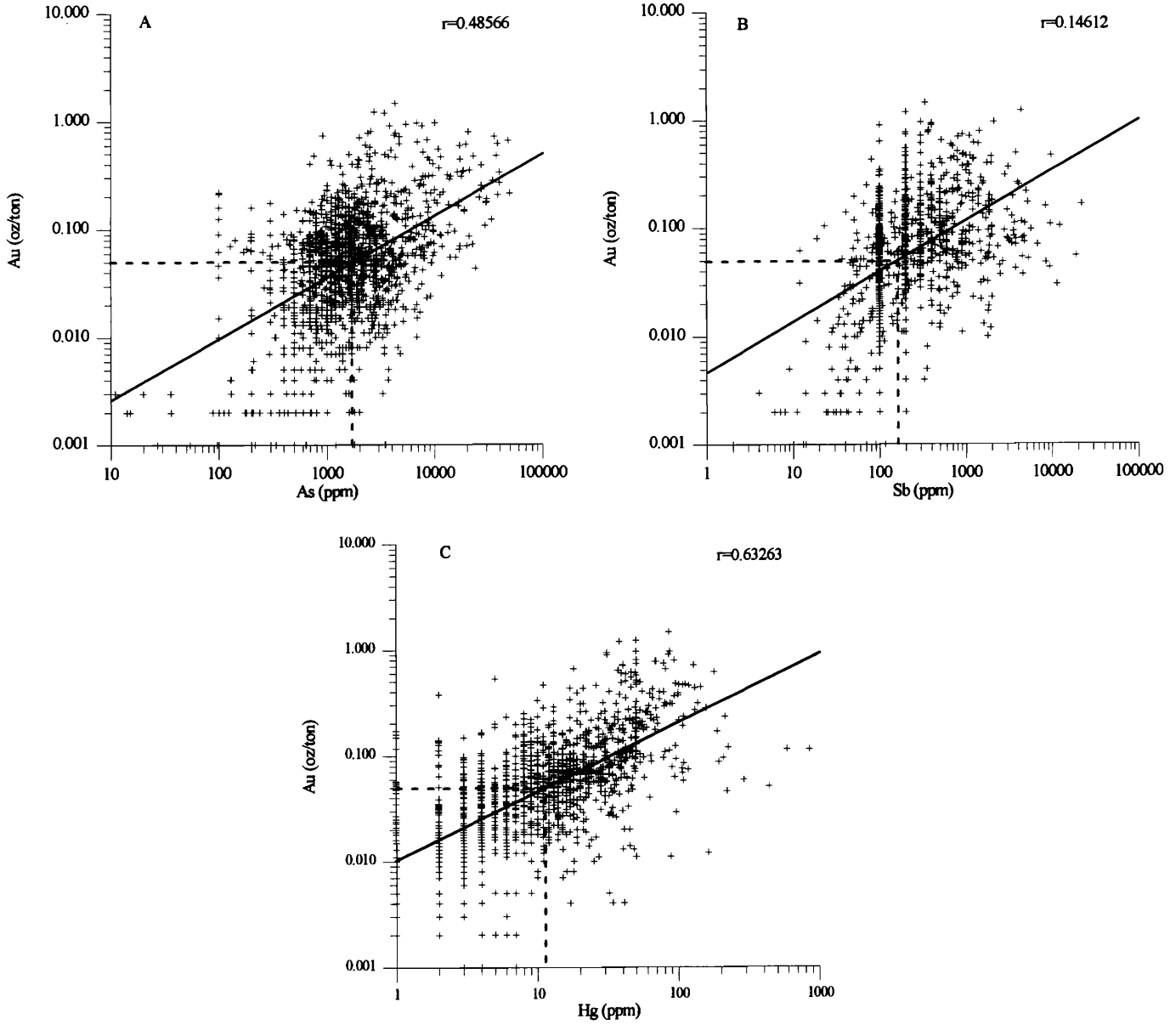

FIG. 7. Relation between gold content of ore samples and their (A) arsenic, (B) antimony, and (C) mercury contents for unoxidized sedimentary rocks in the Ordovician sequence. All figures show best-fit lines for data points along with correlation coefficients. Dashed lines link 0.05 oz/t Au values (which are the outer limits of the gold-rich areas shown in the cross sections) with corresponding values for As, Sb, and Hg and permit evaluation of whether these metals show more or less dispersion than gold.

gold-bearing fluids migrated up smaller structures entering local areas of high fracture permeability.

Distribution of arsenic, antimony, and mercury

Some Carlin-type deposits are enriched in arsenic, antimony, and mercury, although data are scarce on their spatial distribution with respect to gold at the scale of a deposit (Bagby and Berger, 1985). These elements are most commonly present in realgar, orpiment, stibnite, and cinnabar, although significant amounts of arsenic and smaller amounts of antimony and mercury are found in arsenian pyrite (Wells and Mullens, 1973; Arehart et al., 1993). At Twin Creeks, gold in unoxidized ore exhibits positive correlations with As, Sb, and Hg (Fig. 7). Correlation coefficients between gold and these three elements vary greatly, with that for gold and mercury being highest and that for gold and antimony being lowest. The large size of samples included in the tests makes all correlations significant at the 0.01 significance level (Howarth, 1983, p. 400).

The distribution of these elements at Twin Creeks, which is shown in Figure 8 for section B-B′, suggests that antimony is more closely correlated with gold than is mercury or arsenic. As indicated by the dashed line in Figure 7B, gold values of about 0.05 oz/t should correspond to antimony concentrations of about 200 ppm, and Figure 8B shows that this relation is largely valid with the exception of a few high antimony values in gold-poor areas of the upper part of the deposit. Figure 7C shows that gold values of 0.05 oz/t should correspond to mercury concentrations of about 12 ppm. Although this relation is observed in sediments below the main sill, and between the upper sill and the upper tuff, high gold values above the main sill lack high mercury values (Fig. 8C). Figure 7A indicates that gold concentrations of 0.05 oz/t should correlate with arsenic concentrations of about 2,000 ppm. Figure 8A shows that arsenic values of this level are more widely distributed than gold values of 0.05 oz/t. The presence of some gold-poor areas with elevated arsenic values in the upper part of the deposit is consistent with its widespread use as an indicator element in gold exploration.

Relation of Gold to Ore and Alteration Minerals

Gold and carbonate minerals

Dissolution of carbonate minerals is the most common type of rock alteration seen in many Carlin-type deposits. Bakken and Einaudi (1986) and Kuehn and Rose (1992) concluded that gold ore at Carlin was concentrated in moderately silicified zones that had undergone intermediate degrees of carbonate dissolution and that it was found above strongly silicified (jasperoid) feeder structures. Hofstra et al. (1991) reported that most ore in the Jerritt Canyon district is located near but just outside ore-stage jasperoid in zones that underwent carbonate dissolution. High-grade ore zones at Jerritt Canyon show evidence of volume loss due to the removal of carbonate that produced collapse breccias locally (A. Hofstra, written commun., Sept. 1997). At Twin Creeks, the most intense carbonate dissolution in the Etchart formation (exposed in the northern part of the mine area at Chimney Creek) occurs in the center of the orebody, where both dolomite and calcite have been removed (Osterberg, 1990). In peripheral parts of Chimney Creek, only more soluble calcite was dissolved. In sediments of the Ordovician sequence in the Megapit area to the south, Bloomstein et al. (1990) noted that carbonate dissolution increased porosity and permeability in the host rock.

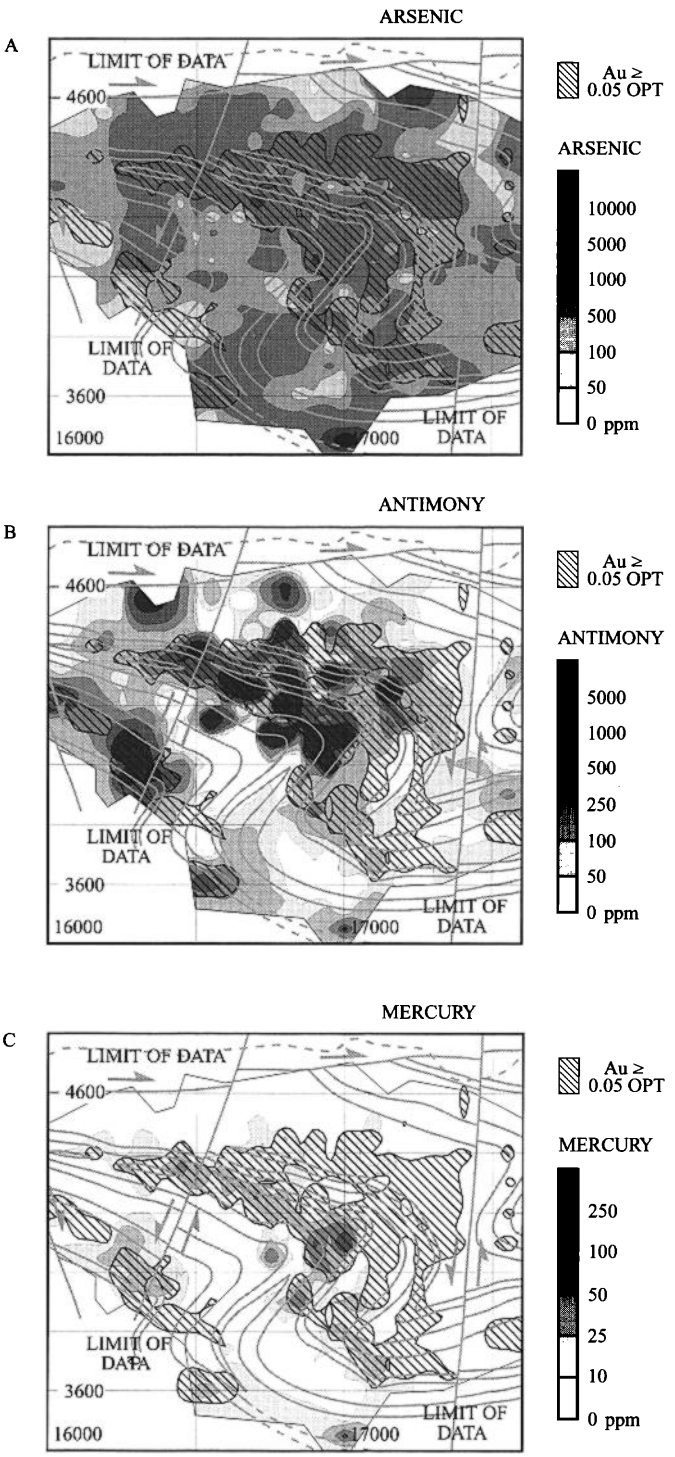

FIG. 8. Distribution of (A) arsenic, (B) antimony, and (C) mercury along section B-B′ showing their relation to gold values, as well as geologic and structural features.

Figure 9 shows the large-scale relation between gold grade and total carbonate in sediments from the Ordovician sequence, as indicated by the bench composite data. Analyses of igneous rocks from the Ordovician sequence, which would have low carbonate contents, are not included in this plot. Samples with high gold grades have low carbonate contents, as is predicted from the alteration studies. Samples with low carbonate contents show a wide range of gold grades. The fact that all samples with low carbonate contents do not have high gold grades suggests that carbonate dissolution was more widespread than gold deposition, although some of this variability could be due to variations in the lithology of the host rocks.

In order to determine the spatial relation between carbonate dissolution and gold mineralization, contoured carbonate data were overlain on geology along the central part of cross section B-B′ (Fig. 10A). This cross section includes only unoxidized samples and confirms that carbonate dissolution is a hypogene alteration feature which is unrelated to acid produced during weathering of the ore. Figure 10A shows that sediments above the upper sill underwent extensive carbonate dissolution and that a smaller area below the main sill was also leached of carbonate. In contrast, sediments between the upper sill and the main sill show relatively little carbonate dissolution. As can be seen in Figure 10A, areas of strongest carbonate dissolution have the highest gold grades. Neither this cross section nor the carbonate-gold plot in Figure 9 provides support for the generalization that gold grades are highest in rocks that have undergone intermediate degrees of carbonate dissolution (Bakken and Einaudi, 1986).

The distribution of carbonate in Figure 10 confirms that structural preparation was not the only control on carbonate dissolution at Twin Creeks. Although the zone of carbonate dissolution in units below the main sill is clearly related to the West Side fault, units between the main and upper sills are along the same structure but did not undergo significant carbonate dissolution. Figure 10B shows variations in the Mg/Ca molar ratio across the central part of cross section B-B′, as compiled from the whole-rock geochemical analyses. Although these samples have a slightly different distribution from those in the bench composite database, it is still clear that the zone of carbonate dissolution below the main sill is partly contained in an area of low Mg/Ca molar ratios, whereas sediments between the main and upper sills have higher Mg/Ca molar ratios. Although Mg/Ca molar ratios in these zones will be modified by dissolution because calcite dissolves more readily than dolomite, these relations suggest that the degree of dissolution also reflects calcite/dolomite ratios in the original sedimentary rock.

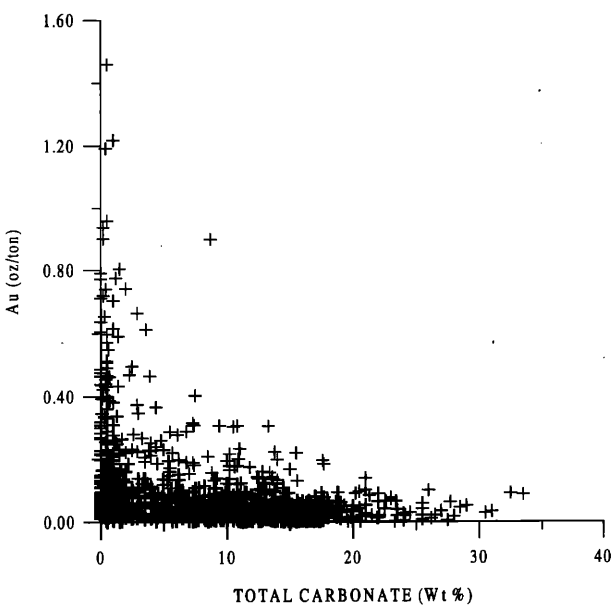

FIG. 9. Gold versus total carbonate (wt %) in unoxidized sedimentary rocks from the Ordovician sequence. Note that gold grades are highest in rocks that have the lowest carbonate contents.

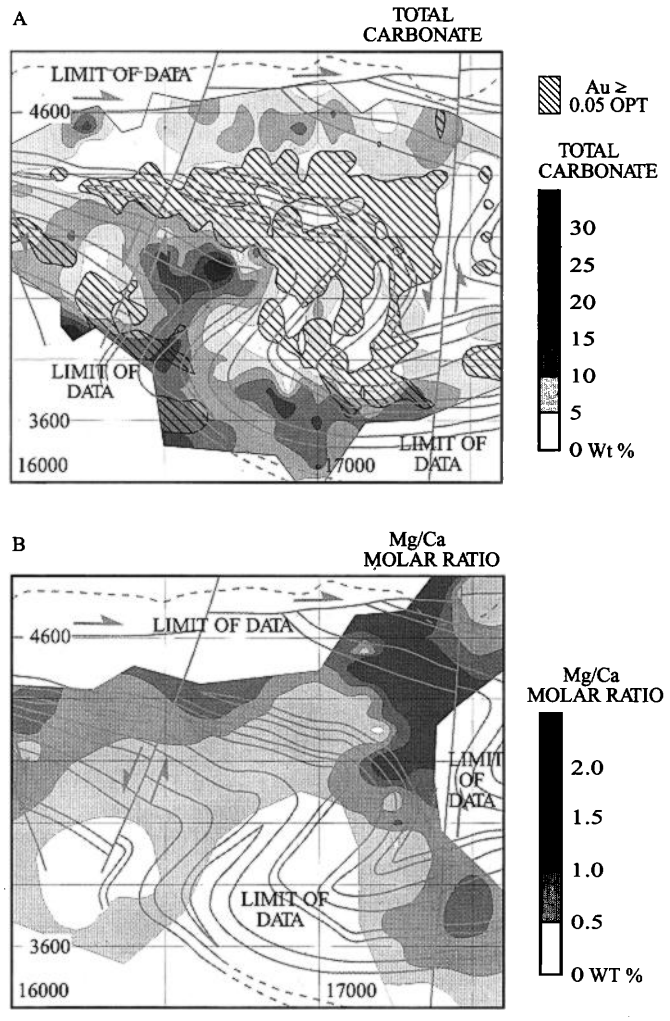

FIG. 10. A. Distribution of carbonate in part of section B-B′. Refer to Figure 2 for names of geologic features. Note that areas of high gold contents (>0.05 oz/t) show good agreement with zones of low carbonate contents. B. Variation in Mg/Ca ratio for part of cross section B-B′. Data for this figure are from a different database from the one used to construct A, but show that carbonate remaining in areas of carbonate dissolution has a high Mg content, consistent with the greater solubility of calcite relative to dolomite.

Gold and silicate alteration minerals

Zoned silicate alteration patterns at Carlin were documented by Kuehn and Rose (1992), who noted that K feldspar

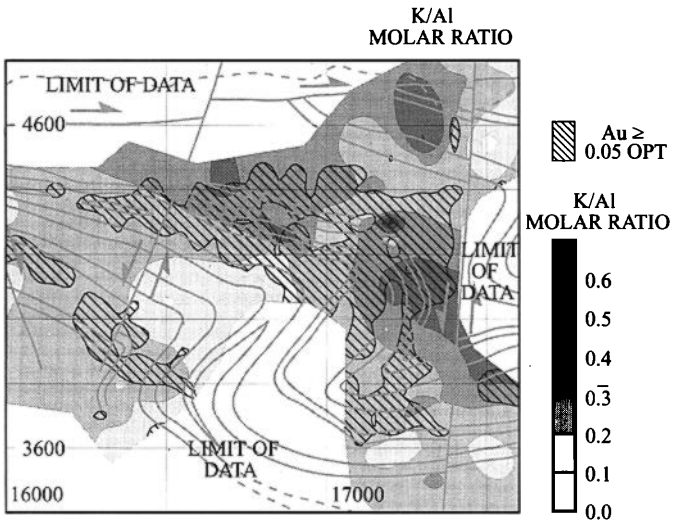

FIG. 11. Plot of K/Al molar ratios of sedimentary rocks of the Ordovician sequence along part of cross section B-B′ showing that the area of high gold values is not enclosed by an area of constant K/Al ratio.

in unaltered calcareous siltstone was altered to potassium-depleted phases toward the center of the hydrothermal system. At Carlin, K feldspar in distal unaltered samples gave way to illite, then to illite-K mica, and finally to kaolinite-dickite at jasperoid feeder zones (Kuehn and Rose, 1992). At Post-Betze, Arehart et al. (1993) found that kaolinite in the core of the hydrothermal system graded into kaolinite-sericite outward toward unaltered rock. In contrast, preservation of detrital illite (Hofstra et al., 1991) suggests that fluids at Jerritt Canyon had a higher K^+/H^+ ratio than those at Carlin, and Drewes-Armitage et al. (1996) reported that 1M illite accompanied deposition of gold at the Genesis and Blue Star mines.

Silicate alteration at Twin Creeks differs from that at most other Carlin-type deposits in containing locally abundant K feldspar, as well as widespread muscovite, especially in the igneous rocks. Adularia is most abundant north of the TC fault where it is clearly intergrown with the first stage of gold-bearing arsenian pyrite and is unquestionably of the same age (Simon et al., 1997, and in prep.). Hall et al. (1997) report a $^{40}Ar/^{39}Ar$ age of 42.1 Ma for this adularia, which agrees with ages reported by Grof et al. (1997). To the south in the direction of the TC fault, as well as along the fault, paragenetically equivalent arsenian pyrite is associated with illite and local kaolinite. Most ore-bearing core material from the area between the feldspar and illite assemblages had been removed for metallurgical testing, making it difficult to determine the exact paragenetic relation between these two assemblages. Later stages of mineralization described above were accompanied only by quartz. Muscovite associated with late orpiment and arsenian pyrite in one area south of the TC fault yields a Paleozoic $^{40}Ar/^{39}Ar$ age and is thought to have formed during metamorphic recrystallization of bentonite(?) layers in the sediment considerably prior to mineralization (Hall et al., 1997).

K and Al abundances in the geochemical database can be used to obtain further insights into the relation between silicate alteration and gold because molar K/Al ratios differ for typical alteration minerals such as K feldspar (1.0), muscovite (~0.333), and kaolinite (0). Sedimentary rocks in the Ordovician sequence at Twin Creeks contain detrital mica and minor feldspar that contribute to the K and Al contents of the rocks, although petrographic examination suggests that there is no significant variation in this original sedimentary silicate mineralogy across the deposit. Thus, contoured K/Al ratios can provide a qualitative indication of the intensity and mineralogy of silicate alteration and its relation to gold. As can be seen in Figure 11, there is no close correspondence between K/Al and gold distribution patterns. Provided there is no systematic variation in original sedimentary mineralogy of these sediments, this relation suggests that gold is not associated directly with a specific silicate alteration mineral such as adularia. This conclusion is supported by relations between Au and K/Al values for all samples from the Megapit area, where it can be seen that high gold values are associated with K/Al ratios of 0.1 to 0.5 (Fig. 12).

Gold and pyrite

Gold in most Carlin-type deposits is closely associated with arsenian pyrite (Wells and Mullens, 1973; Arehart et al., 1993). Simon et al. (1997) have shown that arsenian pyrite has a wide range of morphologies, ranging from coarse-grained, euhedral crystals through fine-grained aggregates to very thin overgrowths on preore pyrite.

Despite our growing understanding of the nature of gold-bearing pyrite, we have less information about deposit-scale relations between pyrite and gold. The Twin Creeks database can be used to test these relations by calculating the abundance of pyrite in samples and comparing it to that of gold. The abundance of pyrite was calculated by determining the amount of sulfide sulfur needed to combine with all arsenic, antimony, and mercury in the sample to make orpiment, stibnite, and cinnabar, respectively, and then determining the amount of iron needed to combine with the remaining sulfide sulfur to make pyrite. This is consistent with analyses indicat-

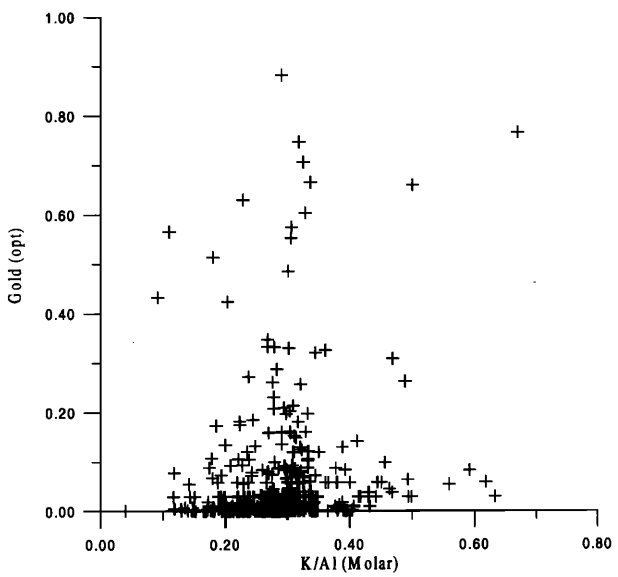

FIG. 12. Relation between Au grade and molar K/Al ratio of sedimentary rocks from the Ordovician sequence in the Megapit area.

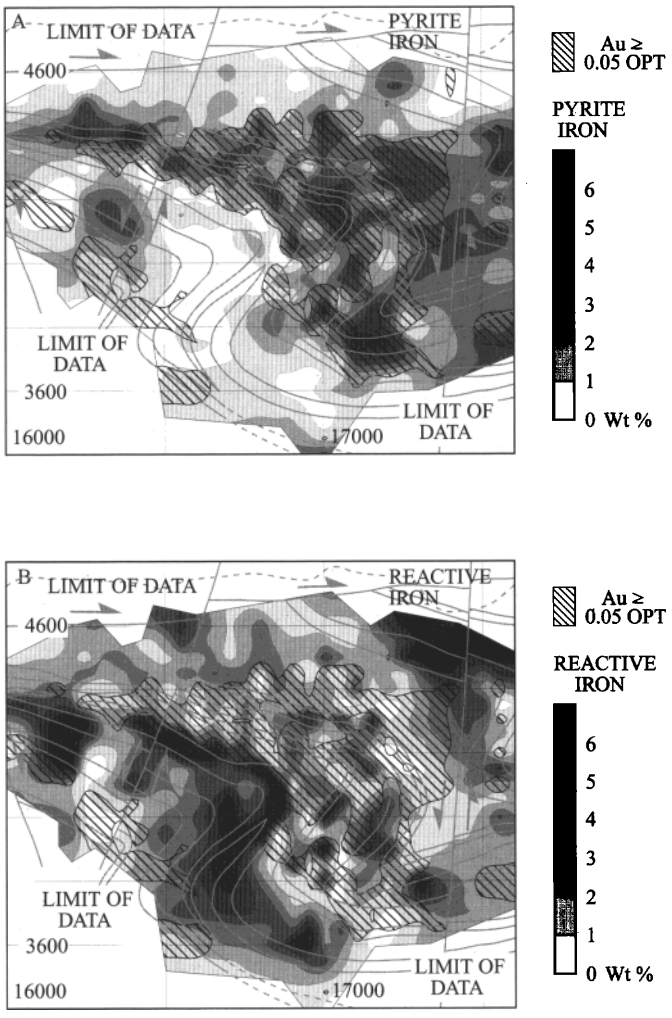

FIG. 13. A. Distribution of pyrite iron calculated by assuming that all reduced sulfur in the analysis is in pyrite or another metal sulfide mineral, as explained in the text, along part of section B-B′. Note the excellent agreement between areas of gold mineralization and areas with abundant pyrite-hosted iron. B. Distribution of reactive iron (i.e., iron not contained in pyrite or another metal sulfide mineral) along part of cross section B-B′. Note that maximum pyrite iron and reactive iron abundances are similar in the two plots (although they reach maximum values inside and outside ore, respectively), indicating that iron was not added to the rock to make pyrite in the mineralized zone. This relation provides strong support for sulfidation as the cause of pyrite and gold deposition.

ing negligible sulfur contents of organic matter in Carlin-type deposits and shales in general (Hausen and Park, 1985; Dean et al, 1987; Raiswell et al., 1993) and the fact that most samples contain more iron than needed to combine with reduced sulfur to make pyrite, as noted below. The abundance of pyrite determined in this way will include both preore sedimentary or diagenetic pyrite and any ore-related pyrite. The relation between gold grade and calculated pyrite abundances along section B-B′ is shown in Figure 13A where pyrite abundance is represented by "pyrite iron," the weight percent iron in the sample that is present in pyrite. The figure shows clearly that areas rich in gold contain the largest amounts of pyrite. This relation supports the textural observations noted above indicating that pyrite forms during mineralization and indicates that ore-related pyrite is more abundant in mineralized areas than preore pyrite.

Cause of Gold Deposition: The Roles of Sulfidation and Decarbonation

The relations shown above provide useful insights into the processes that precipitated gold in Carlin-type deposits. Possible gold-depositing processes include cooling, boiling, fluid mixing and related processes such as dilution or oxidation, and rock-water interaction including processes such as carbonate dissolution, silicate alteration, or sulfidation (Arehart, 1996). All of these processes have found support in recent studies, with an emphasis on fluid mixing and sulfidation. Support for fluid mixing has been provided by data from ore-stage jasperoids at Jerritt Canyon, which indicate a positive correlation between $\delta^{18}O$ values and gold grade (Northrop et al., 1987; Hofstra, 1994). Fluid mixing was also favored by Kuehn and Rose (1995), who suggested that ore was deposited by an acidic, CO_2-rich fluid that escaped from an overpressured environment to mix with cooler, gas-poor meteoric(?) water. Mixing of fluids with different temperatures could also deposit jasperoid and dissolve calcite, two alteration features that are commonly associated with Carlin-type deposits (Fournier, 1985, 1986; Arehart, 1996).

Sulfidation was suggested to be an important gold-depositing process in Carlin-type deposits by Hofstra et al. (1991) and Hofstra (1994) from studies at Jerritt Canyon. Their geochemical modeling showed that fluid mixing and sulfidation could account for gold mineralization, with Fe concentrations of 2 percent in host sediments causing deposition of narrow, high-grade ore zones and lower Fe concentrations of 0.5 percent producing large, low-grade ore zones. Hofstra (1994) noted that the distribution of sulfide minerals in preore dikes at Jerritt Canyon supported the inferred sulfidation process but did not report textural or mineralogical evidence for sulfidation in the sedimentary rocks, which contained most of the ore. In fact, the fact that gold in most Carlin-type deposits is found in arsenian pyrite which forms rims on preore pyrite (Arehart et al., 1993) rather than pseudomorphs after a preore Fe-bearing phase could be interpreted to indicate that pyrite rather than just iron had been introduced to these deposits. Hofstra (oral commun., 1993) noted, however, that iron in the sedimentary rocks could have been liberated during alteration of host rocks to combine almost immediately with introduced sulfur to form pyrite, thus appearing as new pyrite even though only sulfur had been added to the rock.

An early test of this hypothesis was based on a parameter known as the degree of pyritization (DOP), which is defined as: $DOP = Fe_{pyrite}/(Fe_{pyrite} + Fe_{reactive})$, where Fe_{pyrite} refers to iron in pyrite and $Fe_{reactive}$ refers to acid-soluble iron in other phases in the rock (Raiswell et al., 1988). Hofstra (1991, 1994) reported DOP values of 0.7 to 0.9 for sedimentary rocks associated with gold mineralization at Jerritt Canyon compared to values of 0.4 to 0.5 for normal marine sediments (Raiswell et al., 1988). In a further test, Hofstra (1994, fig. 10.21) plotted Au vs. As + S/Fe for mineralized samples from Jerritt Canyon and found that some unweathered samples showed a positive correlation. Although both of these observations were interpreted to support sulfidation as a cause of ore deposition, neither can discriminate between sulfidation

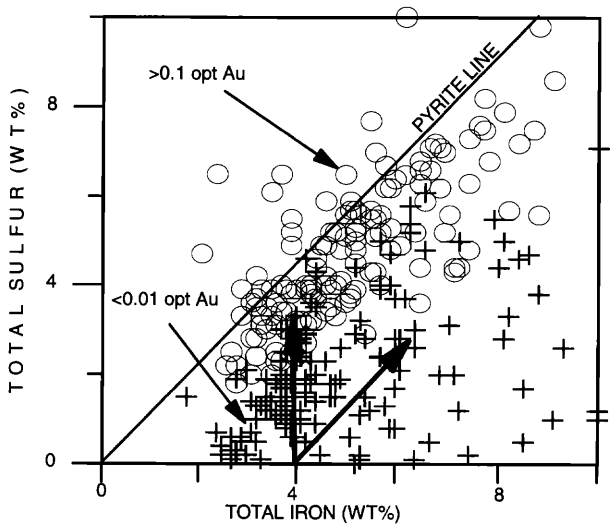

FIG. 14. Weight percent total sulfur versus weight percent total iron for unoxidized sedimentary rocks from the Ordovician sequence. Line shows the Fe/S ratio of pyrite. Note that most samples lie to the right of the pyrite line, showing that the sedimentary rocks contain iron in excess of that bound in pyrite. Symbols represent high-grade (>0.1 oz/t Au) and barren (<0.01 oz/t Au) samples and arrows show direction of compositional change associated with sulfidation (vertical arrow) and with addition of pyrite (diagonal arrow = pyritization). Note that the change in composition from barren to high-grade rocks follows the sulfidation trend.

and introduction of pyrite, both of which cause these values to increase (Kettler et al., 1990, 1992).

Fe-S-Au geochemistry of ore and barren rocks: The role of sulfidation in depositing gold

The question of whether sulfur and iron were introduced into Carlin-type deposits together or independently can be tested effectively with the Twin Creeks geochemical database. Figure 14 shows iron and sulfur contents of Twin Creeks samples along with a line marking the relative concentrations of these elements in pyrite [S = 1.15·Fe (in wt %)]. The distribution of most samples below the pyrite line suggests that the sedimentary rocks contain more iron than is needed to combine with all of their contained sulfur to form pyrite. The relation between iron and sulfur contents and gold grades can be tested further by plotting only samples with gold grades lower than 0.01 oz/t, which represent barren and poorly mineralized rocks, and ore with grades above 0.1 oz/t (Fig. 14). The black arrows in this plot show paths that would be followed on the diagram by samples that underwent sulfidation (addition of only sulfur) or pyritization (addition of sulfur and iron in the ratio typical of pyrite). For samples that undergo sulfidation, displacement parallel to the sulfur axis is limited by the amount of iron available in the sample to combine with sulfur. Complete sulfidation would be achieved at sulfur contents along the pyrite line for the iron content of the sample in question (arsenic, antimony, and other metal sulfides are not abundant enough to complicate this comparison, as can be seen by comparing Figs. 8 and 13). For samples in which pyrite is added, there is no such limit, and at least in theory, iron and sulfur contents can increase until they reach values of 100 percent (e.g. the rock is completely replaced by pyrite). As can be seen in Figure 14, samples with low gold contents (<0.01 oz/t) plot at higher iron and lower sulfur contents than samples with high gold contents (>0.1 oz/t). Although we cannot be certain that the high gold content samples had the same original composition as the low gold samples, the simplest interpretation of these relations is that the process of mineralization involved addition of sulfur, but not iron, to barren rock.

The spatial distribution of gold in relation to the Fe-S chemistry of ore-hosting sediments can be determined by comparing abundances of "pyrite iron," which was calculated as discussed above, and "reactive iron," which represents the weight percent iron in the sample that is not contained in pyrite (rather than acid-soluble iron; Raiswell et al., 1988). These parameters can be compared in Figure 13, which shows clearly that areas of maximum gold concentration coincide with areas of maximum pyrite iron. Even more importantly, it can be seen in Figure 13 that the iron content of ore-bearing rock is the same as the iron content of barren rock outside the ore zone. This relation can only result from sulfidation. Addition of pyrite to these rocks would have resulted in an increase in both iron and sulfur in the ore zone, causing the ore zone to have a higher iron content than surrounding rocks.

Deposition of As, Sb, and H: Sulfidation vs. other processes

Further insights into the role of sulfidation in Carlin-type deposits can be gained from As, Sb, and Hg, which show a distribution generally similar to that of gold, as noted above. Antimony solubility in Carlin-type environments is probably controlled by $HSb_2S_4^-$ and precipitation of stibnite from this complex would be favored by a decrease in the activity of H_2S (Krupp, 1988; Spycher and Reed, 1989). Speciation calculations for mercury in Carlin-type fluids at Jerritt Canyon suggest that HgH_4S_3 and native mercury (Hg^0) were present

TABLE 1. Electron Microprobe Analyses of Dolomite Grains from Ordovician Calcareous Shales

Sample no.	151BC	151BC	151BC	151BC	SED088	SED088	SED088	SED088	SED169
Footage	830.7	830.7	830.7	830.7	706	706	706	706	1295.5
MgO	20.6	20.6	19.1	22.4	18.4	21.2	17.4	20.8	21.8
SrO	0.02	1.45	0.04	0.37	0.45	1.04	0.53	0.18	0.14
CaO	24.8	24.2	21.6	22.1	26.5	23.3	28.5	24.7	25.4
MnO	1.23	0.59	0.54	0.14	2.36	1.67	0.65	0.13	0.94
FeO	9.24	11.6	10.4	15.2	8.53	14.9	10.4	10.0	9.28
C	8.81	9.16	8.69	8.73	8.61	7.79	8.57	7.81	8.40
O	36.6	34.7	34.9	34.4	31.1	34.3	31.2	33.6	35.2
Total	101.6	100.4	98.6	99.2	97.9	101.1	99.9	98.8	100.3

in nearly the same concentrations (Hofstra et al., 1991). Loss of H_2S would cause deposition of cinnabar from HgH_4S_3, but not from Hg^0. Hofstra et al. (1991) concluded that solutions containing Hg^0 can deposit cinnabar if they undergo cooling, oxidation, or pH increase. H_3AsO_3 is the dominant As species at conditions typical of Carlin-type deposits, and a decrease in the activity of H_2S will result in dissolution of realgar and orpiment (Heinrich and Eadington, 1986; Spycher and Reed, 1989). Solubilities of realgar and orpiment are prograde, however, suggesting that cooling would be an effective depositional mechanism, a conclusion also indicated by the reaction-progress calculations of Hofstra et al. (1991).

These comparisons indicate that antimony can be deposited by sulfidation but that deposition of both mercury and arsenic require additional processes. This is consistent with the fact that the distribution of antimony is most similar to that of gold. Fluid mixing that probably accompanies decarbonation, as discussed in the next section, could promote deposition of mercury and arsenic.

Source and availability of iron for sulfidation: The role of decarbonation

Although the geologic relations presented above provide strong evidence that sulfidation was an important agent of gold, and possibly antimony, deposition at Twin Creeks, they do not identify the mineralogical setting of the iron that was sulfidized. Possibilities include oxides, hydroxides, sulfides, carbonates, and silicates, as well as organic matter (Maynard, 1983; Kettler et al., 1990, 1992). Petrographic and microbeam study shows that significant amounts of iron in sedimentary rocks outside the ore zone at Twin Creeks are hosted by diagenetic ferroan dolomite. Electron microprobe analyses indicate that these diagenetic dolomites typically contain about 6 to 12 wt percent iron (Table 1). Figure 9 shows that sedimentary rocks with low gold contents contain about 15 percent CO_3 or about 20 to 25 percent carbonate minerals by weight, depending on whether it is dolomite or calcite. Thus, unmineralized rocks could have contained up to 3 percent Fe in diagenetic ferroan dolomite. Additional iron might have been present in preore rocks as iron oxide coatings on clay minerals, such as those found in deep-sea sediments (Dean and Arthur, 1989), or as fine-grained, iron-bearing chlorite, although it is not likely to have been as easily liberated by mineralizing solutions. In contrast, iron in carbonate minerals would have been readily available, as indicated by the close correspondence between carbonate removal and gold deposition (Fig. 10).

These relations suggest that deposition of gold at Twin Creeks was triggered by dissolution of diagenetic ferroan dolomite, which released iron to form arsenian pyrite. The most effective mechanisms for dissolving most carbonate minerals are cooling or fluid mixing (Fournier, 1985, 1986). As noted above, Northrop et al. (1987) and Kuehn and Rose (1995) have provided geologic and isotopic support for fluid mixing in Carlin-type deposits, and the reaction progress calculations of Hofstra et al. (1991) demonstrate that fluid mixing results in carbonate dissolution. Actual dissolution of carbonate minerals is required to produce the textures seen in Carlin-type ores, specifically the absence of pseudomorphic replacement of ferroan dolomite by arsenian pyrite. By dissolving the ferroan dolomite, the hydrothermal solution would have removed iron from the mineral to react with sulfur from the hydrothermal solution and be deposited almost immediately as arsenian pyrite, thus producing good correspondence between areas of carbonate dissolution and areas of pyrite deposition. The resulting process, in which iron in the wall rock was combined with sulfur from the incoming hydrothermal solution, was clearly a process of sulfidation even though it did not result in pseudomorphic replacement of the iron-bearing mineral.

Conclusions

The results of this study indicate that gold was deposited at Twin Creeks by sulfidation of iron-bearing sedimentary wall rocks. Iron was derived from diagenetic(?) ferroan dolomite and was released during decarbonation. The iron combined with sulfur from the mineralizing solutions to form arsenian pyrite, which caused deposition of gold by decreasing the activity of reduced sulfur in the mineralizing fluid.

This conclusion was derived largely from deposit-scale comparisons based on geochemical data, which provide a different perspective from that obtained in studies based on observations at the scale of hand specimens and outcrops. These comparisons show that gold-bearing solutions at Twin Creeks were introduced along faults but that large amounts of gold were deposited away from these faults in favorable lithologies. Comparison of the distribution of gold relative to other important metals in Carlin-type deposits shows that antimony has a distribution similar to that of gold, whereas arsenic is more widely dispersed than gold and mercury is more concentrated than gold. These comparisons show further that gold is most abundant in areas of greatest carbonate removal, that there is no strong correlation between gold and K silicate mineralogy, that gold is most concentrated in areas with the highest pyrite contents, and that total iron contents in ore zones are not different from those in adjacent barren rocks. These relations can only be explained if iron in the original rock was converted to pyrite by the addition of sulfur (along with gold and other metals) from the mineralizing solution.

Our results indicate that decarbonation, an important form of alteration in most Carlin-type deposits, can cause gold deposition by releasing iron, which is deposited as pyrite in a modified form of sulfidation. This suggests that exploration for Carlin-type deposits could be guided by delineation of sedimentary rocks rich in diagenetic ferroan carbonate minerals.

Acknowledgments

This study could not have been carried out without the whole-hearted support of the geology staff of the Santa Fe Pacific Gold Corporation. In addition to providing generous guidance and discussion, they provided complete access to drill logs, geologic correlations, chemical analyses, petrographic data, and thin sections obtained by their geology team over a period of many years. At the mine, we were helped by Bob Kastelic, Jerry Willis, Clay Postlethwaite, Sherry Weiber, Vic Ridgely, Kirk Rentmeister, Don MacKerrow, Ron Parker, Al Berry, Ron Kieckbush, Warren Tompson, Dave MacLean, Mark Whitney, Greg Hill, and Rich Parrish. Others in the Santa Fe organization helped arrange for our work and provided financial support, including Ken Sageser, Ron Parratt,

Roy Owen, Bob Felder, and Ed Bloomstein, who was instrumental in starting the outstanding databases on which our work was based. We have also benefited from discussions, field visits, or laboratory sessions with Greg Arehart, Eric Essene, John Fortuna, Joe Graney, Chris Hall, Al Hofstra, Jim O'Neil, K.C Lohmann, Grigore Simon, and Ed Van Hees. Research at Twin Creeks was supported by National Science Foundation grant EAR95-23771 to S.E.K.; electron microbeam work was carried out with equipment obtained under National Science Foundation grants EAR82-12764 and BSR83-1402. The original manuscript was improved by helpful reviews from two *Economic Geology* referees.

June 24, December 5, 1997

REFERENCES

Arehart, G.B., 1996, Characteristics and origin of sediment-hosted disseminated gold deposits: A review: Ore Geology Reviews, v. 11, p. 383–403.

Arehart, G.B., Chryssoulis, S.L., and Kesler, S.E., 1993, Gold and arsenic in iron sulfides fromsediment-hosted disseminated gold deposits: Implications for depositional processes: ECONOMIC GEOLOGY, v. 88, p. 171–185.

Bagby, W.C. and Berger, B.R., 1985, Geologic characteristics of sediment-hosted, disseminated precious-metal deposits in the western United States: Reviews in Economic Geology, v. 2, p. 169–202.

Bakken, B.M., and Einaudi, M.T., 1986, Spatial and temporal relations between wall-rock alteration and gold mineralization, main pit, Carlin gold mine, Nevada, *in* Macdonald, A.J., ed., Gold '86: Willowdale, Ontario, Konsult International, p. 388–403.

Bakken, B.M., Hochella, M.F., Jr., Marshall, A.F., and Turner, A.M., 1989, High-resolution microscopy of gold in unoxidized ore from the Carlin mine, Nevada: ECONOMIC GEOLOGY, v. 84, p. 171–179.

Bloomstein, E. I., Massingill, G.L., Parratt, R.L., and Peltonen, D.R., 1990, Discovery, geology, and mineralization of the Rabbit Creek gold deposit, Humboldt County, Nevada, *in* Raines, G.L., Lisle, R.E., Schafer, R.W., and Wilkinson, W.H., eds., Geology and ore deposits of the Great Basin: Reno, Geological Society of Nevada, p. 821–843.

Cline, J.S., Hofstra, A., Landis, G. and Rye, R.O., 1997, Ore fluids at the Getchell, Carlin-type gold deposit, north-central Nevada: Society of Economic Geologists Field Trip Guidebook, v. 28, p. 155–166.

Dean, W.E., and Arthur, M.A., 1989, Iron-sulfur-carbon relationships in organic-carbon-rich sequences I: Cretaceous Western interior seaway: American Journal of Science, v. 289, p. 708–743.

Dean, W.E., Pratt, L.M., Brigg, P.H., Daws, T.A., Engleman, E.E., Jackson, L., Layman, L.R., Ryder, J.L., Stone, C.L., Threlkeld, C.N., and Vuletich, A.K., 1987, Data on the geochemistry of Carlin-type disseminated gold deposits and associated rocks, north-central Nevada: U.S. Geological Survey Open-File Report 87–446, 19 p.

Drewes-Armitage, S.P., Romberger, S.B., and Whitney, C.G., 1996, Clay alteration and gold deposition in the Genesis and Blue Star deposits, Eureka County, Nevada: ECONOMIC GEOLOGY, v. 91, p. 1383–1393.

Fournier, R.M., 1985, Silica minerals as indicators of conditions during gold deposition: U.S. Geological Survey Bulletin, v. 1646, p. 15–26.

—— 1986, Carbonate transport and deposition in the epithermal environment: Reviews in Economic Geology, v. 2, p. 63–72.

Groff, J.A., 1996, Geochronology and origin of auriferous fluids for the Getchell and Twin Creeks mines, Humboldt Country, Nevada: Unpublished Ph.D. dissertation, Socorro, New Mexico Institute of Mining and Technology, 291 p.

Groff, J.A., Heizler, M.T., McIntosh, W.C., and Norman, D.I., 1997, $^{40}Ar/^{39}Ar$ dating and mineral paragenesis for Carlin-type gold deposits along the Getchell trend, Navada: Evidence for Cretaceous and Tertiary gold mineralization: ECONOMIC GEOLOGY, v. 92, p. 601–622.

Hall, C.M., Simon, G., and Kesler, S.E., 1997, Age of mineralization at the Twin Creeks SHMG deposit, Nevada: Society of Economic Geologists Field Trip Guidebook, v. 28, p. 151–153.

Hausen, D.M., and Park, W.C., 1985, Observations on the association of gold mineralization with organic matter in Carlin-type ores, *in* Dean, W.E., ed., Organics and ore deposits, Proceedings of the Denver Region Exploration Geologists Society Symposium: Denver, Denver Region Exploration Geologists Society, 218 p.

Heinrich, C.A., and Eadington, P.J., 1986, Thermodynamic predictions of the hydrothermal chemistry of arsenic and their significance for the paragenetic sequence of some cassiterite-arsenopyrite-base metal sulfide deposits: ECONOMIC GEOLOGY, v. 81, p. 511–529.

Hofstra, A.H., 1994, Geology and genesis of the Carlin-type gold deposits in the Jerritt Canyon district, Nevada: Unpublished Ph.D. dissertation, University of Colorado, Boulder, 719 p.

Hofstra, A.H., Leventhal, J.S., Northrop, H.R., Landis, G.P., Rye, R.O., Birak, D.J., and Dahl, A.R., 1991, Genesis of sediment-hosted disseminated-gold deposits by fluid mixing and sulfidation: Chemical-reaction-path modeling of ore-depositional processes documented in the Jerritt Canyon district, Nevada: Geology, v. 19, p. 36–40.

Hotz, P.E., and Willden, R., 1964, Geology and mineral deposits of the Osgood MountainsQuadrangle Humboldt County, Nevada: U.S. Geological Survey Professional Paper 424B, 128 p.

Howarth, R.J., ed., 1983, Statistics and data analysis in geochemical prospecting: Handbook of exploration geochemistry: Elsevier, Amsterdam, v. 2, 431 p.

Kettler, R.M., Waldo, G.S., Penner-Hahn, J.E., Meyers, P.A., and Kesler, S.E., 1990, Sulfidation of organic matter associated with gold mineralization, Pueblo Viejo, Dominican Republic: Applied Geochemistry, v. 5, p. 237–248.

Kettler, R.M., Rye, R.O., Kesler, S.E., Meyers, P.A., Polanco, J. and Russell, N., 1992, Gold deposition by sulfidation of ferrous Fe in the lacustrine sediments of the Pueblo Viejo district (Dominican Republic): The effect of Fe-C-S diagenesis on later hydrothermal mineralization in a maar-diatreme complex: Chemical Geology, v. 99, p. 29–50.

Krupp, R.E., 1988, Solubility of stibnite in hydrogen sulfide solutions, speciation, and equilibrium constants, from 25 to 350°C: Geochimica Cosmochimica Acta, v. 52, p. 3005–3015.

Kuehn, C.A., and Rose, A.W., 1992, Geology and geochemistry of wall-rock alteration at the Carlin gold deposit, Nevada: ECONOMIC GEOLOGY, v. 87, p. 1697–1721.

——1995, Carlin gold deposits, Nevada: Origin in a deep zone of mixing between normally pressured and overpressured fluids: ECONOMIC GEOLOGY, v. 90, p. 17–36.

Maynard, J.B., 1983, Geochemistry of sedimentary ore deposits: Berlin, Springer-Verlag, 303 p.

Northrop, H.R., Rye, R.O., Landis, G.P., Lustwerk, R., Jones, M.B., and Daly, W.E., 1987, Sediment-hosted disseminated gold mineralization at Jerritt Canyon. V—Stable isotope geochemistry and a model of ore deposition [abs.]: Geological Society of America Abstracts with Programs, v. 19, p.791.

Osterberg, M. W., 1990, Geology and geochemistry of the Chimney Creek gold deposit, Humboldt County, Nevada: Unpublished Ph.D. dissertation, University of Arizona, 173 p.

Raiswell, R., Buckley, F., Berner, R.A., and Anderson, T.F., 1988, Degree of pyritization of iron as a paleoenvironmental indicator of bottom-water oxygenation: Journal of Sedimentary Petrology, v. 58, p. 812–819.

Raiswell, R., Bottrell, S.H., Al-Biatty, H.J., and Tan, M.M., 1993, The influence of bottom water oxygenation and reactive iron content on sulfur incorporation into bitumens from Jurassic marine shales: American Journal of Science, v. 293, p. 569–596.

Radtke, A.S., Rye, R.O., and Dickson, F.W., 1980, Geology and stable isotope studies of the Carlin gold deposit, Nevada: ECONOMIC GEOLOGY, v. 75, p. 641–672.

Rye, R.O., 1985, A model for the formation of carbonate-hosted disseminated gold deposits based on the geologic, fluid-inclusion, geochemical, and stable-isotope studies of the Carlin and Cortez deposits, Nevada: U.S. Geological Survey Bulletin 1646, p. 35–42.

Simon, G., Kesler, S.E., Chryssoulis, S., Huang, H., and Penner-Hahn, J.E., 1997, Preliminary data on pyrite textures and the mineralogy of gold at Twin Creeks SHMG deposit, Nevada [abs.]: Society of Economic Geologists Field Trip Guidebook, v. 28.

Spycher, N.F., and Reed, M.H., 1989, As(III) and Sb(III) sulfide complexes: An evaluation of stoichiometry and stability from existing experimental data: Geochimica et Cosmochimica Acta, v. 53, p. 2185–2194.

Stenger, D.P., 1996, Chemical and isotopic zoning at the Twin Creeks sediment-hosted micron gold deposit, Nevada: Unpublished M.Sc. thesis, University of Michigan, 76 p.

Stewart, J.H., 1980, Geology of Nevada: Nevada Bureau of Mines and Geology Special Publication 4, 136 p.

Wells, J.D., and Mullens, T.E., 1973, Gold-bearing arsenian pyrite determined by microprobe analysis, Cortez and Carlin gold mines, Nevada: ECONOMIC GEOLOGY, v. 68, p. 187–201.